25 October, 2005

Final Technical report, "Extension of Electromagnetic Code for Phased Array Analysis and Design", EOARD Grant Number FA8655-05-1-3054

Abstract

This is a final report for EOARD grant number FA8655-05-1-3054, "Extension of electromagnetic code for phased array analysis and design". The name of the electromagnetic code is PB-FDTD. The unique property of the code is that it can perform unit cell analysis of periodic structures (such as array antennas) in the time domain. This means that a broadband response is obtained in a single computation. The antenna element feed is a key part of phased array antennas. An accurate model for the feed is therefore important. Some type of feeds can already be modeled in the PB-FDTD code. Waveguide ports are very common in array antennas. Such feeds have however not been implemented in the PB-FDTD code. The main objective of the work was therefore to implement waveguide port in the PB-FDTD code. This has been accomplished. Another objective was to simplify the analysis of arrays with circular polarized antenna element. This and more have been done. The code can now calculate both the polarization and the transmission coefficient to all propagating Floquet modes. The GUI for the code has also been modified in order to handle the new functions.

Background

Many electromagnetic problems have a periodic structure. Examples are phased array antennas, frequency selective surfaces (important for stealth application), meta-materials (currently a hot research area) and electromagnetic bandgap materials. Electromagnetic analysis and design of such structures are greatly simplified by the use of a mathematical theorem called Floquets theorem [1]. With Floquets theorem only one unit cell in the periodic structure needs to be modeled. The electromagnetic interaction to all other unit cells is automatically taken into account. Previously, unit cell analysis based on Floquets theorem was always performed in the frequency domain. This means that only one frequency point at the time can be analyzed. In many cases, a broadband response is required (for example radar cross section calculations and broadband array design). A time domain version of Floquets theorem is therefore highly desirable since that would generate data for all frequencies in a single computation. A time domain version of Floquets theorem was developed by Henrik Holter during his PhD-studies 1997-2000 [2]. The new method has been implemented in the very popular Finite-Difference Time-Domain method (FDTD) for solving Maxwells equations. The name of the computer code is PB-FDTD (Periodic Boundary FDTD). The use of FDTD means that complicated structures and materials can be modeled. Some years ago, EOARD supported the development of a graphical user interface etc (GUI) for the PB-FDTD code under contract no. F61775-00-WE037. The PB-FDTD code has after that continuously been improved. It can now handle all the periodic structures mentioned above. The code is numerically highly efficient and has proved quite useful at the AFRL, Hanscom, MA and other places.

REPORT DOCUMENTATION PAGE	Form Approved OMB No. 0704-0188

1. REPORT DATE ***(DD-MM-YYYY)***	**2. REPORT TYPE**	**3. DATES COVERED** *(From – To)*
18-11-2005	Final Report	1 August 2005 - 01-Feb-06

4. TITLE AND SUBTITLE Extension of Electromagnetic Code for Phased Array Analysis and Design	**5a. CONTRACT NUMBER** FA8655-05-1-3054
	5b. GRANT NUMBER
	5c. PROGRAM ELEMENT NUMBER
6. AUTHOR(S) Dr. Henrik P Holter	**5d. PROJECT NUMBER**
	5d. TASK NUMBER
	5e. WORK UNIT NUMBER
7. PERFORMING ORGANIZATION NAME(S) AND ADDRESS(ES) Henrik P Holter Korsuddsvagen 17B Nacka Sweden	**8. PERFORMING ORGANIZATION REPORT NUMBER** N/A
9. SPONSORING/MONITORING AGENCY NAME(S) AND ADDRESS(ES) EOARD PSC 802 BOX 14 FPO 09499-0014	**10. SPONSOR/MONITOR'S ACRONYM(S)**
	11. SPONSOR/MONITOR'S REPORT NUMBER(S) SPC 05-3054

12. DISTRIBUTION/AVAILABILITY STATEMENT

Approved for public release; distribution is unlimited.

13. SUPPLEMENTARY NOTES

14. ABSTRACT

Theoretical analysis and computer simulation of electrical feeds for antenna arrays and waveguides. The aim will be to establish propagation characteristics associated with antenna feeds, and establish reliable computer models for each type of feed.

15. SUBJECT TERMS

EOARD, Radiofrequency radiation, Electromagnetics, Antennas

16. SECURITY CLASSIFICATION OF:			**17. LIMITATION OF ABSTRACT**	**18, NUMBER OF PAGES**	**19a. NAME OF RESPONSIBLE PERSON** MICHAEL KJ MILLIGAN, Lt Col, USAF
a. REPORT UNCLAS	**b. ABSTRACT** UNCLAS	**c. THIS PAGE** UNCLAS	UL	16	**19b. TELEPHONE NUMBER** *(Include area code)* +44 (0)20 7514 4955

Standard Form 298 (Rev. 8/98)
Prescribed by ANSI Std. Z39-18

Objective

The PB-FDTD code has primarily been used for broadband phased array antenna design (several scientific papers have been published in periodicals where the PB-FDTD code has been used). The feed is a key part of array antennas and therefore needs to be included in the computer model. Some type of feeds (coaxial cables, micro-strip lines and striplines) can already be modeled in the PB-FDTD code. However one of the most common feeds in array antennas, waveguide ports, cannot be modeled. The main proposed research effort is therefore to implement waveguide ports in the computer code. That would make the code still more useful. Waveguides are complicated since the electromagnetic field inside the guide is described by a sum of forward and backward traveling propagating and non-propagating modes. The shape and frequency dependent propagation constant of the modes depend on the waveguide cross-section and the material inside the guide and must in general be calculated numerically. The waveguide must be terminated in a load that absorbs all backward traveling propagating and non-propagating modes. Further, the use of waveguide modes together with unit cell technique caused an intricate problem that had to be solved (described later in the text).

An additional part of the proposal is to simplify the analysis of arrays with circular polarized antenna elements. For characterization of such elements with the current code, several computations with subsequent post-processing are necessary. The proposed research effort is to simplify this.

Statement of work

The proposed services in the application to EOARD are described in this section.

The waveguide implementation consists of the following parts:

- The cross-section of the waveguide can be circular or rectangular. These are the most common shapes. The code will almost certainly handle almost arbitrary cross-sections, but that can not be guaranteed. (It turned out that the code can handle arbitrary cross-sections).
- The waveguide can be filled with a lossless dielectric material.
- The waveguide feed is directed in the array normal direction.
- The number of waveguide modes can be specified by the user. The code automatically calculates the modes and sorts them after the value of the associated transversal wavenumber.
- The user specifies which of the modes that excite the guide.
- The coupling between the exited mode and the other waveguide modes is automatically calculated.
- For degenerated modes, the user can specify any linear combinations of such modes in order to control the polarization.
- A unit cell in the array contains one waveguide feed. More than one waveguide feed will probably bee implemented, but that can not be guaranteed.
- Examples with waveguide feeds is included in the manual for the code
- The array lattice is rectangular. Attempts will be done to implement waveguide feeds for triangular lattices also.

- The waveguides can also be used for scattering (RCS) calculations. A plane wave incident on the array is used for that.

The circular polarized element analysis part consists of the following parts:

- Simplification of the calculation of the scattering parameters between the antenna element and the zero order TE- and TM-mode Floquet modes. It is accomplished in the following way: the antenna is excited and the coupling to the zero order TE- and TM-modes is calculated. (It turned out that the coupling to all, not only the zeros order, propagating Floquet modes is calculated).
- An example in the manual.

In addition to the above, the graphical user interface (GUI) will be updated so it can handle the new functionalities.

Deliverables

- Computer code, inclusive source code (FORTRAN and MATLAB).
- Updated manual. New examples.

Implementation of waveguide ports

In this section, the implementation of waveguide ports in the PB-FDTD code is described in detail.

There are several ways to implement waveguide ports in the FDTD method. Some research has therefore been carried out in order to find the most accurate and usable method. The workload for implementing the method has not been a constraint. The chosen method is described in [3]. It is a mod-matching technique.

Since a mode matching technique is used, evanescent modes can be included in the expansion of the field in the waveguide. This means that the port does not need to be very long in order to correctly handle evanescent modes.

There are two steps in order to implement the mod-matching technique. First the waveguide modes, transversal wave-numbers and the time domain impulse response of each mode must be determined. Second, the waveguide modes together with the impulse responses are used to truncate and excite the waveguide in the FDTD method. These two steps are described below.

Waveguide modes

Since the waveguide cross section can have an almost arbitrary shape, the waveguide modes must be determined numerically (as a matter of fact, even if the waveguide where rectangular, using the known theoretical modes and wave-numbers would result in inaccurate results. This has to do with the mesh in FDTD). In order to find the modes, Helmholtz's two-dimensional equation for the longitudinal part of the electric or magnetic field or Laplace equation for the potential is solved together with suitable boundary conditions.

$$\begin{aligned}&\left(\nabla^2 + k_T^2\right)H_Z = 0, \text{TE - modes}\\&\left(\nabla^2 + k_T^2\right)E_Z = 0, \text{TM - modes}\\&\nabla^2 V = 0, \text{TEM - modes}\end{aligned} \tag{1}$$

The boundary conditions are

$$\begin{aligned}&\frac{\partial H_Z}{\partial n} = 0, \text{TE - modes}\\&E_Z = 0, \text{TM - modes}\\&V \text{ constant on each conductor, different on different conductors}\end{aligned} \tag{2}$$

Solving (1) on the FDTD-mesh results in a matrix. For TE- and TM-modes, the eigenvalues and eigenvectors of this matrix correspond to the transversal wave-numbers squared and the longitudinal magnetic or electric field. For TEM-modes, the potential in the waveguide cross section is obtained.

The transversal electric field is needed for the mode matching technique. For TE- and TM-modes the transversal field is obtained via Maxwell's equations. For TEM-modes, the electric field is obtained from the gradient of the potential

$$\overline{E}_T = -\nabla V \tag{3}$$

Equation (1) is solved on the same mesh as the FDTD-mesh. That guarantees that the accuracy will be high. Observe that (1) is a frequency domain equation for the modes. The modes are however the same in the time domain.

Construction of the matrix above for arbitrary waveguide cross-sections and taking into account the boundary condition turned out to be a complex task. A MATLAB and a FORTRAN program have been developed for this part.

The time domain impulse response of the waveguide modes is also required for the mode matching technique. In [3], it is showed how the impulse responses can be calculated numerically by a recursive formula. This method has been used here.

Implementation in FDTD

In this section, the implementation of the mode matching technique in the FDTD method is described step by step.

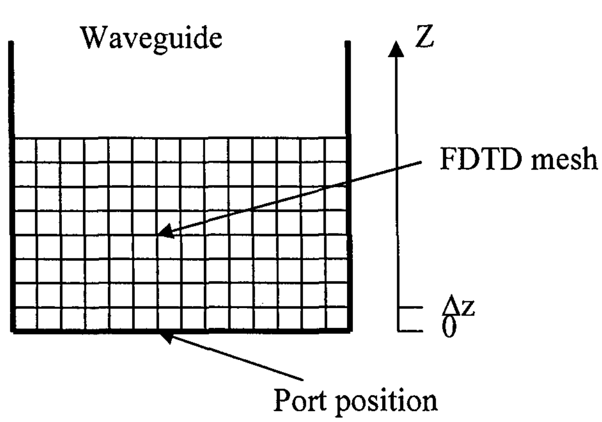

Figure 1. Waveguide example. Side view.

The electric field in the waveguide cross-section at $z=0$ in Figure 1 is going to be computed from the known electric field in the cross-section at $z=\Delta z$ and the incident signal at $z=0$. Applying the computed field at $z=0$ will both truncate and excite the waveguide. The truncation is in theory reflection free. Examples later in this report show that the reflection is very small.

Assume that the FDTD cell size in the z-direction is given by Δz and the discrete time t_k in the FDTD method is given by

$$t_k = k\Delta t\,, \tag{4}$$

where Δt is the FDTD time step.

The total transversal electric field at $z = \Delta z$ can be expressed as an expansion of N orthonormalized waveguide modes (evanescent modes can be included)

$$\overline{E}_T(\Delta z, k\Delta t) = \sum_{n=1}^{N} a_n(k\Delta t)\overline{e}_n \tag{5}$$

$\overline{E}_T(\Delta z, k\Delta t)$ is a known quantity (from the FDTD method). The voltage a_n is determined from orthogonality

$$a_n(k\Delta t) = \int_S \overline{E}_T(\Delta z, k\Delta t)\cdot\overline{e}_n ds,\quad n = 1..N \tag{6}$$

To obtain the backward voltages, $a_{-,n}$, the incident voltage needs to be subtracted from the a_n.

Assume that the incident signal at $z=0$ is given by $s(t)$ and that mode m is the source (incident) waveguide mode.

The incident signal at $z=\Delta z$ is given by the convolution between $s(t)$ and the waveguide impulse response for mode m.

$$s_{\Delta z}(k\Delta t) = P_m(k) * s(k\Delta t) = \sum_{q=1}^{k-1} s(q\Delta t)P_m(k-q) \tag{7}$$

The impulse response P_m is calculated according to [3].

The backward voltages at $z=\Delta z$ is given by

$$a_{-,n}(k\Delta t) = \begin{cases} a_n(k\Delta t) - s_{\Delta z}(k\Delta t),\, n = m \\ a_n(k\Delta t),\, n \neq m \end{cases},\quad n = 1..N \tag{8}$$

The backward voltages at $z=0$ is given by the convolution between the $a_{-,n}$ and the impulse response.

$$a_{-,n}^{z=0}(k\Delta t) = P_n(k) * a_{-,n}(k\Delta t) = \sum_{q=1}^{k-1} a_{-,n}(q\Delta t)P_n(k-q),\quad n = 1..N \tag{9}$$

Next, the voltages of the total field at $z=0$ is calculated by adding the incident signal $s(t)$ to (9)

$$a_n^{z=0}(k\Delta t)=\begin{cases} a_{-,n}^{z=0}(k\Delta t)+s(k\Delta t), n=m \\ a_{-,n}^{z=0}(k\Delta t)\, n\neq m \end{cases}, \quad n=1..N \tag{10}$$

The total transversal field at $z=0$ is finally given as a superposition of waveguide modes

$$\overline{E}_T(z=0,k\Delta t)=\sum_{n=1}^{N} a_n^{z=0}(k\Delta t)\overline{e}_n \tag{11}$$

This field is applied at the plane $z=0$ in the FDTD-code. As a result, backward traveling modes will be absorbed at $z=0$ (if they are included in the N modes). At the same time, the excitation signal $s(t)$ is applied at $z=0$.

The above steps are repeated for each time step in the FDTD method. The method requires that all $a_{-,n}(k\Delta t)$ and $a_n^{z=0}(k\Delta t)$ is saved for all FDTD time steps k. Memory is also required to save the impulse response for each waveguide mode and the excitation signal. The memory requirement for all this is however small compared with the memory requirement for the FDTD mesh.

Some remarks on the shape of the excitation signal $s(t)$: The spectrum of the pulse should have an energy distribution that is adapted to the desired frequency range. It is very common to use a Gaussian pulse in the FDTD method. A waveguide however has a cut-off frequency. The pulse should therefore contain little energy below and near the cut-off frequency. Otherwise, very long simulation times caused by slowly propagating signals just above the cut-off frequency may occur. In the literature, people have suggested to use a sinc-pulse in the time domain (square pulse in the frequency domain) for waveguide excitation in the FDTD method. This has been tried here. It was however found that such pulses caused some problems. One problem is that the shape of the sinc-pulse in the time domain decay slowly ($1/t$). Since a truncated sinc-pulse must be used in the FDTD method, the Fourier transform will not be a perfect square. And it will therefore be energy below the cut-off frequency. Second, using a sinc-pulse with the unit-cell technique in PB-FDTD sometimes resulted in numerical instabilities. The reason for that is again that a truncated sinc-pulse must be used (the sinc-pulse is not very small when the computation starts). A Gaussian pulse has an exponential decay in both the time- and the frequency domain. This is much better for the unit cell technique. A Gaussian pulse is therefore used in PB-FDTD for excitation of waveguides. When the user specifies the frequency range in PB-FDTD, the start frequency should not be below the cut-off frequency.

Mode matching and the PB-FDTD unit cell technique

The mode matching technique require that the field in the cross-section of the waveguide at $z=\Delta z$ is available. This result in a difficulty for the unit cell technique in PB-FDTD. The unit cell technique, described in [4], is based on a unit cell that during the computation is moved over the periodic structure (for example an array antenna) with at least the speed of light. This is illustrated in Figure 2 where each unit cell has a circular waveguide. The dark unit cell in Figure 1 is the unit cell modeled in FDTD. It is that unit cell that is moved over the surface during the computation.

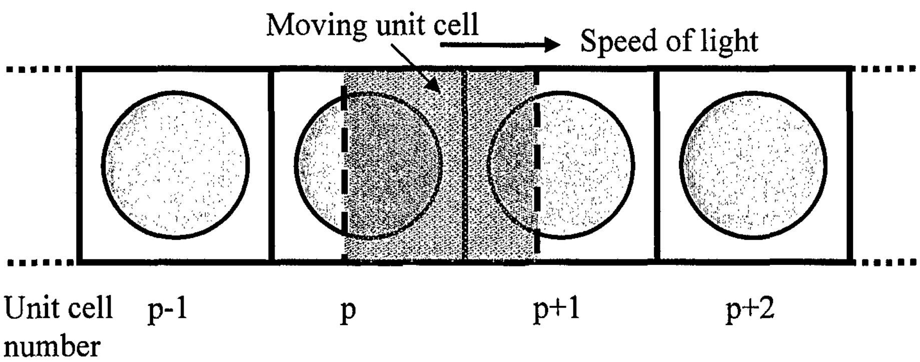

Figure 2. Unit cell technique. A moving unit cell is used. The circle in each unit cell is a waveguide port.

From equation (6) in the mode matching technique, it is obvious that the transversal field in the waveguide at $z=\Delta z$ is needed. The problem is that according to Figure 2, only a part of the waveguide may be inside the moving unit cell (it is not possible just to combine the two partial visible waveguides in the moving unit cell in Figure 2 since there is a time shift between them). The total transversal field in the waveguide cross section at $z=\Delta z$ is therefore not available at all FDTD time steps.

A non-approximate solution for this intricate dilemma was however found. The solution to the problem is first to use two instead of one moving unit cell, see Figure 3. That guarantees that a whole waveguide is visible for a sufficient long time. Second, the partially visible waveguide in unit cell p+1 in Figure 3 still constitute a problem. The total transversal field at $z=\Delta z$ is not available. So it is not possible to calculate the $a_{-,n}(k\Delta t)$ and $a_n^{z=0}(k\Delta t)$ from (6)-(10). That is however not needed since these values have already been calculated for the waveguide in unit cell p at time $k\Delta t - \delta t$. The time δt is related to the scan angle, θ_0, the element spacing, d, and the speed of light c_0.

$$\delta t = \frac{d \sin\theta_0}{c_0}. \tag{11}$$

This solves the problem. So as long as the rightmost waveguide is just partially visible in the moving unit cell, $a_{-,n}(k\Delta t)$ and $a_n^{z=0}(k\Delta t)$ are obtained from the waveguide to the left of this waveguide at an earlier time step.

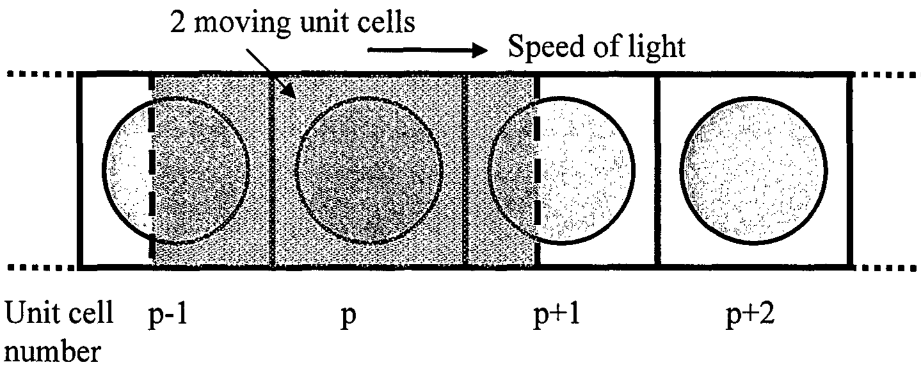

Figure 3. Two unit cells modeled in FDTD.

Frequency domain data

Frequency domain data is obtained via a Fourier transform of the backward traveling voltages $a_{-,n}^{z=0}(k\Delta t)$ and the in-signal $s(t)$.

The coupling between the excited waveguide mode, m, and all other waveguide modes is calculated as

$$S_{nm} = \frac{\sqrt{Z_n}}{\sqrt{Z_m}} \frac{V_n}{V_m}, n = 1..N, \tag{12}$$

where V_n are the frequency domain modal voltages. V_m is the Fourier transform of the in-signal $s(t)$. Z_n and Z_m are the wave-impedances of mode n and m. The wave impedance is calculated from the transversal wave-number, k_T, which is obtained when equation (1) is solved.

$$\begin{aligned} Z_{TE} &= \frac{k_T}{\omega\mu} \\ Z_{TM} &= \frac{\omega\varepsilon}{k_T} \\ Z_{TEM} &= \frac{\omega}{c} \end{aligned} \tag{13}$$

Normalization with the square root of the wave-impedances in (12) results in generalized scattering parameters.

Examples

Examples with waveguide ports have been added to the manual for the PB-FDTD software. One example is a phased array with ridged waveguides radiating into free space. Results from this example are shown below. The fundamental mode is shown in Figure 4 (all modes can be plotted in the PB-FDTD code). The generalized scattering parameters are shown in Figure 5. A comparison between PB-FDTD and Ansoft HFSS is shown in Figure 6 and Figure 7. Ansoft HFSS is a popular commercial frequency domain code that can handle periodic structures. Since it is a frequency domain code, it must redo the calculation for each frequency point of interest.

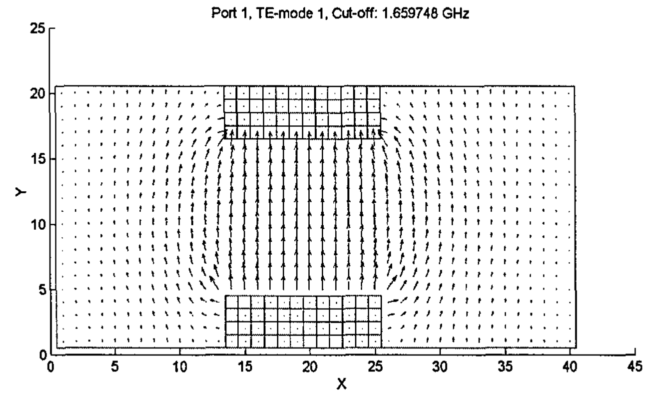

Figure 4. Fundamental mode in the waveguide.

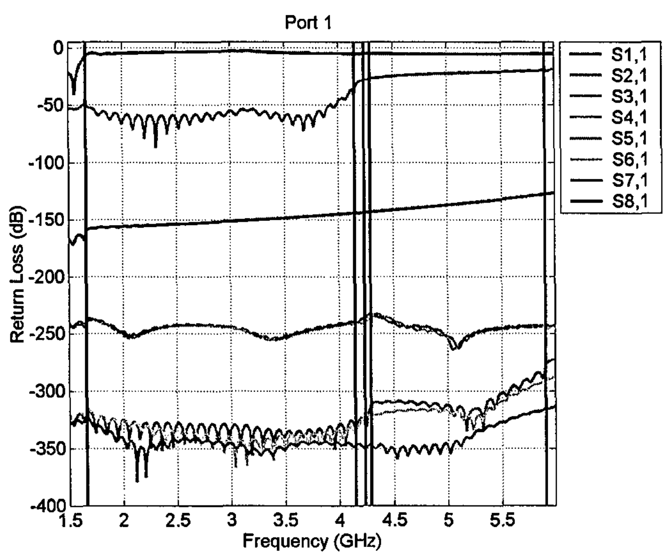

Figure 5. S-parameters. Mode 1 is the source mode. Scan angle: 45 degrees in the H-plane. The vertical lines indicate when higher order modes in the waveguide start to propagate.

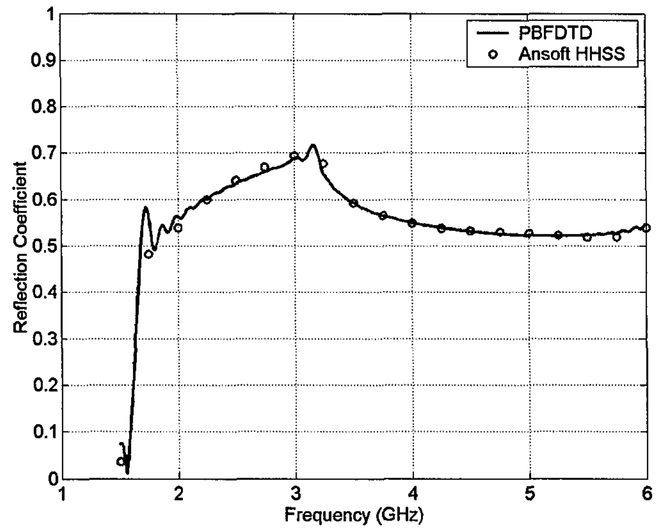

Figure 6. Magnitude of S_{11}. Comparison with Ansoft HFSS. Scan angle: 45 degrees in the H-plane. First grating lobe at 3.2 GHz.

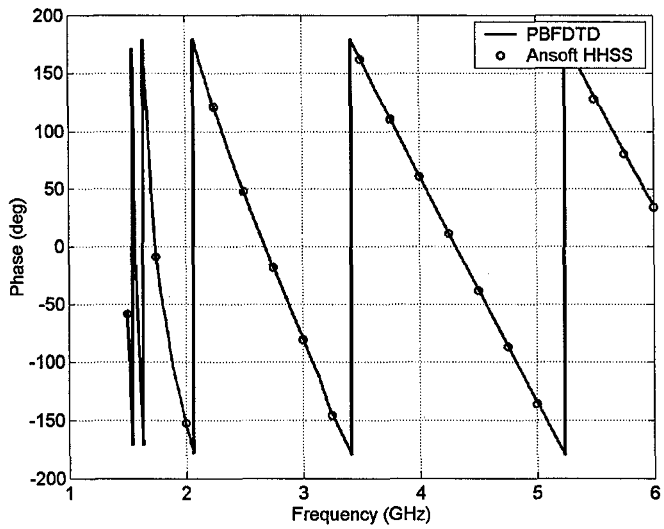

Figure 7. Phase of S_{11}.

The next example is an air-filled rectangular waveguide that instead of radiating into free space is terminated in a short. The inner dimension of the waveguide is 48.75×22.5 mm. The length of the guide is 25 mm. The frequency range has been set to 1-10 GHz.

6 TE-modes and 2 TM-modes are used. TE-mode 1 is the source mode. Below are the calculated cut-off frequencies for the modes:

Mode 1, TE-mode: 1, Cut-off: 3.156995 GHz
Mode 2, TE-mode: 2, Cut-off: 6.308597 GHz
Mode 3, TE-mode: 3, Cut-off: 6.658208 GHz
Mode 4, TE-mode: 4, Cut-off: 7.368742 GHz
Mode 5, TE-mode: 5, Cut-off: 9.172248 GHz
Mode 6, TE-mode: 6, Cut-off: 9.449421 GHz

Mode 7, TM-mode: 1, Cut-off: 7.368742 GHz
Mode 8, TM-mode: 2, Cut-off: 9.172248 GHz

The calculated scattering parameters are shown in Figure 8 - Figure 10. The coupling from TE-mode 1 to higher order modes should in theory be zero. Because of numerical noise, there is always a finite coupling. As can be seen in Figure 8, the coupling is very small (< -250 dB). The vertical lines in the figures indicate where higher order modes start to propagate in the waveguide (the cut-off frequencies above).

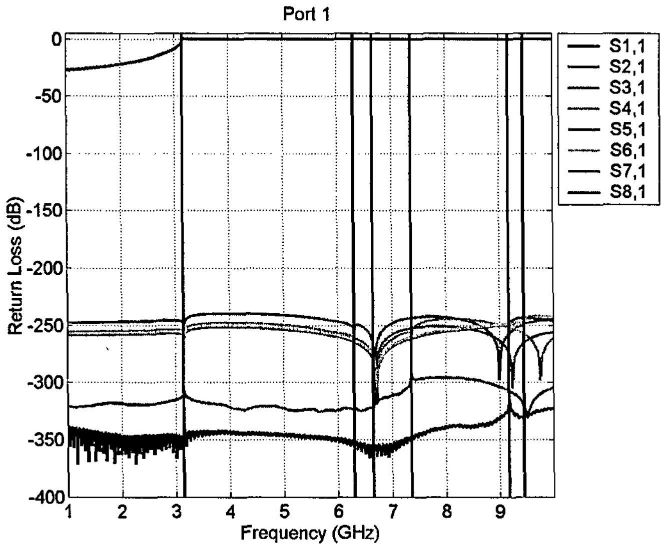

Figure 8. S_{11} - S_{82}.

S_{11} is shown in Figure 9 and Figure 10. S_{11} should in theory be equal to 0 dB (total reflection because of the short. As can be seen in the figures, S_{11} is very close to 0 dB. In Figure 9, the Return Loss does not go directly to zero at the cut-off frequency (3.16 GHz) of the first TE-mode. This is almost certainly because of very slowly propagating signals at frequencies close to the cut-off frequency.

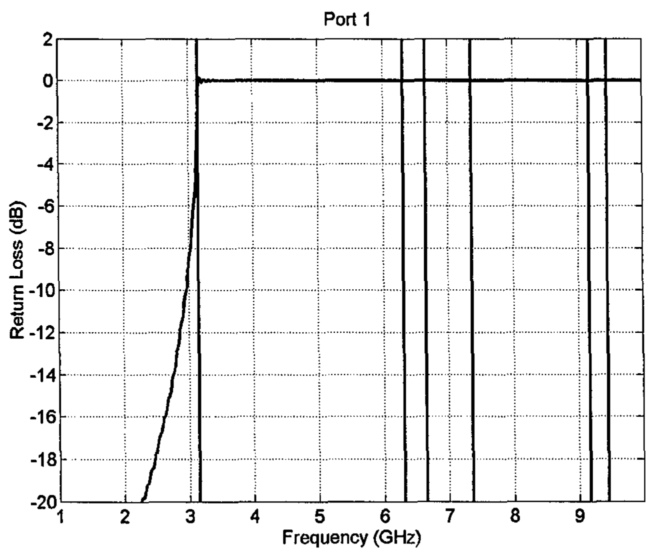

Figure 9. S_{11}.

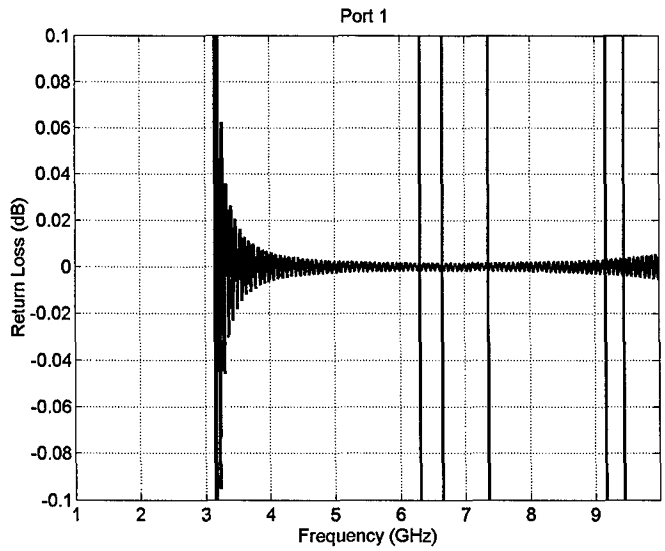

Figure 10. S_{11}. Observe the scale on the y-axis.

Third example: calculated return loss for a single polarized Vivaldi-array scanned to 30 degrees in the H-plane is shown in Figure 11. The element is fed by a stripline. This TEM-type of transmission line could already be modeled with another (less advanced, more lengthy) technique in PB-FDTD. The agreement between the two methods in Figure 11 is very good.

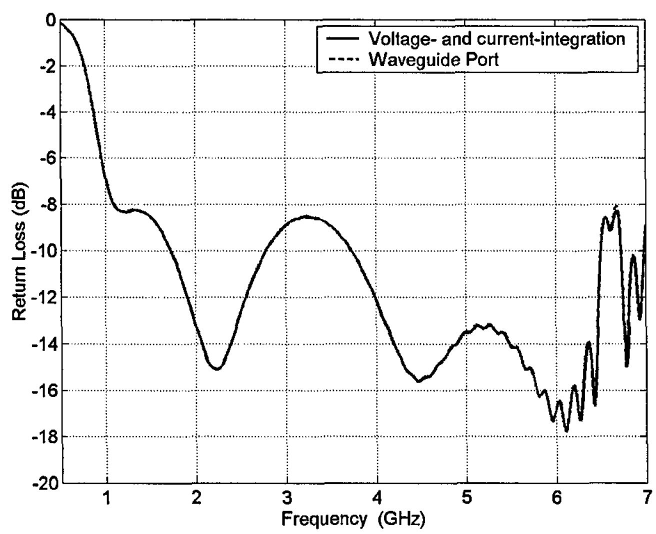

Figure 11. Return loss of an array with Vivaldi-elements. Two different feed techniques.

The Vivaldi-element and the stripline port TEM-mode is shown in Figure 12 and Figure 13.

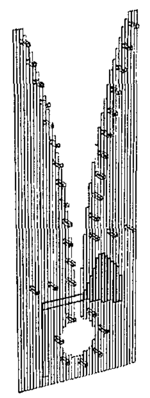

Figure 12 A tapered slot element with plated through vias (one of the metal fins has been removed to increase the visibility). The element is fed by a stripline.

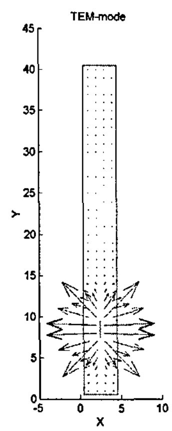

Figure 13. Calculated stripline port TEM-mode. Electric field in the cross-section is shown.

Polarization and transmission coefficient

Two parameter of considerable interest in phased array antennas is the polarization and the transmission coefficient between the antenna feed and the Floquet modes. Calculation of these parameters has been implemented in the PB-FDTD code.

The original objective, as mentioned earlier in the report, was to simplify the analysis of arrays with circular polarized antenna element. The implementation here is more general than that.

Polarization

The polarization is presented in the form of magnitude and phase of the electric field components for all propagating Floquet modes. An example (dual polarized Vivaldi phased array scanned into the diagonal plane) from the PB-FDTD manual is shown in Figure 14 and Figure 15 (no higher order propagating modes).

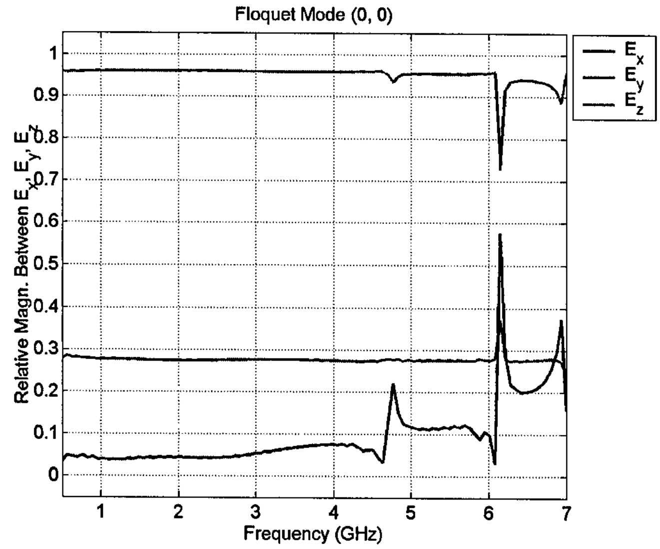

Figure 14. Polarization. Relative magnitude between the electric field components.

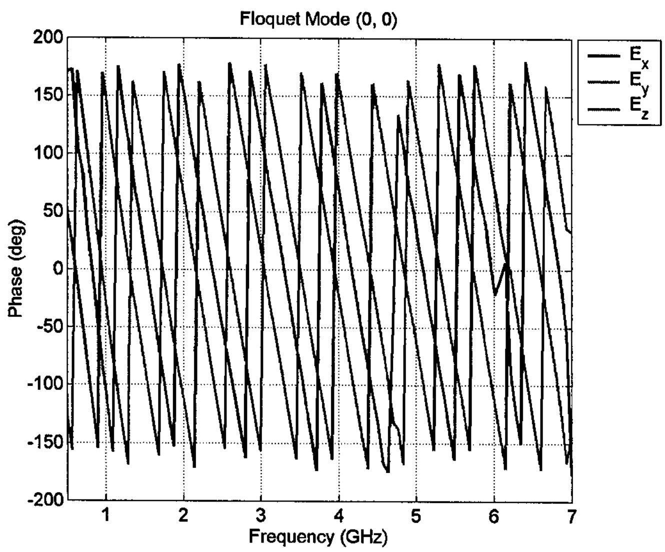

Figure 15. Polarization. Phase of the electric field components.

Transmission coefficient calculation

The transmission coefficient between an antenna feed and all propagating Floquet modes is calculated according to the following equation

$$T_{x(y)}^{m,n} = \frac{\sqrt{Z_{Floquet}^{m,n}}}{\sqrt{Z_{Antenna}}} \frac{V_{Floquet}^{m,n}}{V_{Antenna}} \tag{14}$$

$Z_{Floquet}^{m,n}$ is the wave impedance of Floquet mode (m,n)

$Z_{Antenna}$ is the source impedance. For point sources: equal to the internal resistance. For waveguide ports: equal to the wave-impedance of the excited mode.

$V_{Floquet}^{m,n}$ is the amplitude of the normalized Floquet mode (m,n)

$V_{Antenna}$ is the in-signal to point sources or waveguide ports.

Normalization with the square root of the wave-impedances in (14) results in generalized scattering parameters.

In PB-FDTD, structures are periodic in the xy-plane. The z-direction is normal to the surface of the periodic structure. The transmission coefficient in (14) is calculated for the coupling to the x- and y-components of the electric field of the Floquet modes.

For loss-free array antennas, experiment calculations have shown that energy conservation is satisfied (a necessary but not sufficient condition for proving that everything is correct).

$$|\Gamma_A|^2 + \sum_n |T_x^{m,n}|^2 + \sum_n |T_y^{m,n}|^2 = 1, \tag{15}$$

where Γ_A is the array active reflection coefficient. The summation is over all propagating Floquet modes.

An example (dual polarized Vivaldi phased array scanned into the diagonal plane) from the PB-FDTD manual is shown in Figure 16 (no higher order propagating modes).

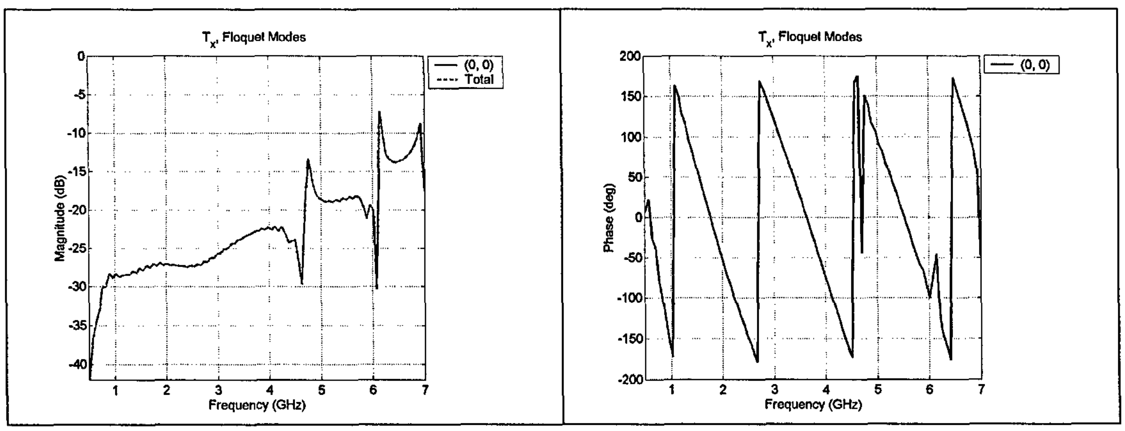

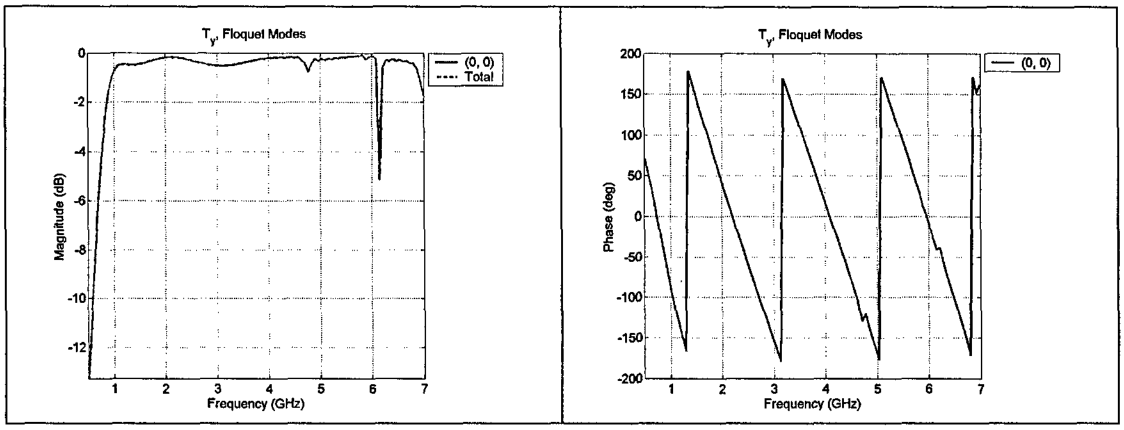

Figure 16. Transmission coefficient, magnitude and phase.

Conclusions

More than all of the proposed services in the statement of work have been fulfilled. It was promised that rectangular and circular waveguides should be implemented. The code can actually handle waveguides with arbitrary cross-section. It can also handle waveguides with TEM-modes (ex. coaxial cables and striplines).

It was also stated that analysis of circular polarized antenna elements should be simplified. The implementation in the code is more general than that (the polarization and transmission coefficient calculation).

There is a graphical user interface (GUI) for the code. The GUI has been modified in order to handle the new functions.

References

[1]. Amitay, Galindo and Wu, "Theory and analysis of phased array antennas", ISBN 0-471-02553-4.

[2]. Henrik Holter, "Analysis and design of broadband phased array antennas", PhD-thesis, Royal Inst. of Technology, May 2000.

[3]. F. Alimenti et.al., "A revised formulation of modal absorbing and matched modal source boundary condition for the efficient FDTD analysis of waveguide structures", IEEE Transactions on Microwave and Techniques, No. 1, January 2000, pp. 50-59.

[4]. H. Holter and H. Steyskal, 'Infinite phased array analysis using FDTD periodic boundary conditions-pulse scanning in oblique directions', IEEE Transactions on Antennas and Propagation, October 1999, pp. 1508-1514.